REPORT DOCUMENTATION PAGE

Form Approved
OMB No. 0704-0188

PLEASE DO NOT RETURN YOUR FORM TO THE ABOVE ORGANIZATION.

1. REPORT DATE *(DD-MM-YYYY)*	2. REPORT TYPE	3. DATES COVERED *(From - To)*
02-29-2012	Final Report	July 1, 2009 - Nov. 30, 2011

4. TITLE AND SUBTITLE
FIRST KINETIC SIMULATIONS OF EQUATORIAL SPREAD-F - ANALYSIS OF KILOMETER-TO-METER SCALE IRREGULARITIES

5a. CONTRACT NUMBER
FA9550-09-1-0402

5b. GRANT NUMBER

5c. PROGRAM ELEMENT NUMBER

6. AUTHOR(S)
Meers Oppenheim, Yann Tambouret, and Yakov Dimant

5d. PROJECT NUMBER

5e. TASK NUMBER

5f. WORK UNIT NUMBER

7. PERFORMING ORGANIZATION NAME(S) AND ADDRESS(ES)
Boston University
85 E Newton St M-921
Boston MA 02118-2436

8. PERFORMING ORGANIZATION REPORT NUMBER

9. SPONSORING/MONITORING AGENCY NAME(S) AND ADDRESS(ES)
USAF, AFRL DUNS 143574726
AF Office of Scientific Research
875 N. Randolph St. Room 3112
Arlington VA 22203

10. SPONSOR/MONITOR'S ACRONYM(S)

11. SPONSOR/MONITOR'S REPORT NUMBER(S)
AFRL-OSR-VA-TR-2012-0998

12. DISTRIBUTION/AVAILABILITY STATEMENT
General Distribution/Unclassified

Distribution A: Approved for Public Release

13. SUPPLEMENTARY NOTES

14. ABSTRACT
This AFOSR project investigated the small-scale ($<$ 100 m) plasma dynamics of Convective Ionospheric Storms (CEIS), i.e. Equatorial Spread-F. CEIS cause sever degradation of earth-to-satellite communication signals (e.g. GPS) and other disruptions of communication. Our plan was to investigate the dynamics of small-scale CEIS using Particle-in-Cell (PIC) simulations and theory. All previous simulations had used large-scale fluid codes which generally ignored the important physics that occurs at scale sizes below 100 m. In order to do this, we developed our existing massively-parallel PIC simulator, adding new boundary conditions and field solvers. We then performed 2 and 3 dimensional simulations initialized with strong density gradients. We found that these gradients result in small scale drift wave instabilities perpendicular to the background density gradient. The gradient length scales required to produce these instabilities, however, are slightly smaller than those previously measured in situ by satellites and rockets. We conclude that a simple drift wave instability is sufficient to explain the development of small scale irregularities as they quickly dissipate the steepened structures that drive their growth. We are currently preparing a manuscript discussing these results.

15. SUBJECT TERMS
Plasma Dynamics, CEIS, Spread-F, Earth-Space Communication, GPS, Simulations, PIC

16. SECURITY CLASSIFICATION OF:			17. LIMITATION OF ABSTRACT	18. NUMBER OF PAGES	19a. NAME OF RESPONSIBLE PERSON
a. REPORT	b. ABSTRACT	c. THIS PAGE			Meers Oppenheim
U	U	U	UU		19b. TELEPHONE NUMBER *(Include area code)* 617-353-6139

1 Introduction

The focus of this AFOSR sponsored research project is to investigate the small-scale (< 100 m) plasma dynamics of Convective Equatorial Ionospheric Storms (CEIS), i.e. Equatorial Spread-F. CEIS are challenging to predict, and they cause debilitating degradation of earth-to-satellite communication signals (e.g. GPS). The instabilities at the smallest length scale are essential for rationalizing the existence of coherent radar echos of CEIS, and these instabilities provide the energetic sink for the large scale dynamics, commonly called spread-F bubbles. Little direct evidence exists to identify the specific driving force responsible for developing these waves, and several proposed theories for their growth mechanism fail to address all length scales [Huba and Ossakow, 1979, 1981a,b]. Our objective was to develop a better understanding of this physics by simulating it using Particle-in-Cell (PIC) codes.

PIC simulators model small-scale, non-linear, and kinetic effects, which the large-scale fluid-based simulations cannot study. However, PIC codes cannot explore large-scale or slowly evolving systems. Nevertheless, we used such a code to investigate 2 and 3 dimensional systems initialized with strong density gradients. We found that these gradients resulted in small scale drift wave instabilities perpendicular to the background density gradient. The gradient length scales required to produce these are slightly smaller than those previously measured in situ by satellites and rockets. Therefore, we conclude that a simple drift wave instability is sufficient to explain the development of small scale irregularities so long as they quickly dissipate the steepened structures that drive their growth. We found that the third dimension (dynamics parallel to the background magnetic field, $\mathbf{B}$) resulted in subtly different dynamics. Since the dynamics developed much slower parallel to $\mathbf{B}$, the 2 dimensional simulations, perpendicular to $\mathbf{B}$, produced qualitatively similar short-time dynamics and the 2D simulations are still very relevant. We also performed exploratory studies into the combined driver of local electric fields and density gradients. We are currently preparing a manuscript discussing these results.

While these PIC simulations are well suited to accurately describe the physics at these small scales, the calculations are computationally costly compared to fluid-based models. Considerable effort for this project was directed towards improving the capabilities of our PIC simulator to better

suit it for these large simulations. The major update involved adding the capability non-periodic simulations, where the flux of particles at one simulation boundary differed from the opposite boundary. This ability made it possible to sustain, essentially indefinitely, density gradients across the simulation. The fact that this new code is parallelized is also important, because it allows us to harness the efficiency of some of the worlds largest super computers and to simulate for larger length scales and longer times. We also implemented a quasi-neutral solver that treats the electrons as an inertialless fluid which responds instantly to the ion density while maintaining $\nabla \cdot \mathbf{J} = 0$. While this formulation has less sever numerical constraints, it is much more difficult to parallelize.

2 Detailed Discussion

Density gradients play an essential role in driving CEIS, and they are the main source of energy for the largest scale irregularities. As in situ measurements have verified, steep local density gradients exist following the development of spread-F bubbles. The spectra of density irregularities perpendicular to the magnetic field differ horizontally vs. vertically, and particularly sharp gradients (gradient length scales–$n(\nabla n)^{-1}$, approaching 50 m) have been measured vertically [Singh and Szuszczewicz, 1984]. The theory of collisional interchange instability explains this steepening preferentially along the vertical direction [Kelley et al., 1987]. Hysell et al. [1994] showed that for a simple model of these waves, parallel to the background density gradient (typically the vertical direction) they lead to steepened intermediate scale (100-1000 m) structures with very sharp gradients. It is clear from measurement and theory that these steep intermediate scale gradients exist, and it is these structures (and their associated fields) we hypothesize predominately drive the small scale irregularities.

2D simulations Our 2D simulations were oriented perpendicular to the magnetic field and encompassed approximately 2500 m^2. Since the time to develop the intermediate scale structures (nearly 15 minutes) is much longer then can be physically modeled using PIC simulations, we initialize the system with a density gradient comparable to that which would be produced by another process, such as the collisional interchange instability [Hysell et al., 1994]. In the direction perpen-

Parameters		Value
$\delta x, \delta y$	m	0.06
Nx		1024
Ny		512
δt	s	2.4e-06
$B_0 \cdot \hat{z}$	G	2.500e-05
nproc		256
$L = n(\lvert\nabla n\rvert)^{-1}$	m	7.680e+00
n_0	m^{-3}	3.078e+08
T_0	K	1.000e+03
m_e	kg	9.100e-29
$N_{particle,\,e}$		5.244e+07
ν_n	s^{-1}	0.000e+00
Cyclotron frequency, Ω_e	s^{-1}	4.401e+04
Larmour radius, a_e	m	2.799e-01
m_i	kg	2.600e-26
$N_{particle,\,i}$		1.049e+08
n_0	m^{-3}	3.078e+08
Cyclotron frequency, Ω_i	s^{-1}	1.540e+02
Larmour radius, a_i	m	4.731e+00

Table 1: **Simulation Parameters**

dicular to the gradient ($\hat{y}$), we used periodic boundary conditions while parallel ($\hat{x}$) we use more a range of non-periodic boundary conditions, discussed below. Table 1 shows the parameters used to initialize simulator. We used values typical of nighttime F-region conditions, with two exceptions: The peak density is the lowest value typically found during the nighttime. With this value, the plasma Debye length is largest, resulting in the most efficient simulation possible. Comparison runs at larger densities produced similar results. Secondly, the electron mass is larger than the physical value, and this too is chosen to maximize computational resources. Using heavy electrons is a common approach in PIC simulations, and we stayed within suggested limits [Dimant and Oppenheim, 2004]. The electron's mass's effect was studied and is discussed below.

In such a system one would expect diamagnetic drifts to develop, where ions drift upward and electrons downward. This drives a drift wave instability, which has been studied extensively [Gary, 1993]. This instability, and similar variants, are stable for the weak gradients that drive the large scale CEIS dynamics [Huba and Ossakow, 1981b], but the standard analysis assumes that

the gradient length scale $(n(\nabla n)^{-1})$ exceeds the ion Larmour radius. This assumption fails for the steep structures we used. Figure 1 shows a typical evolution of the ion density.

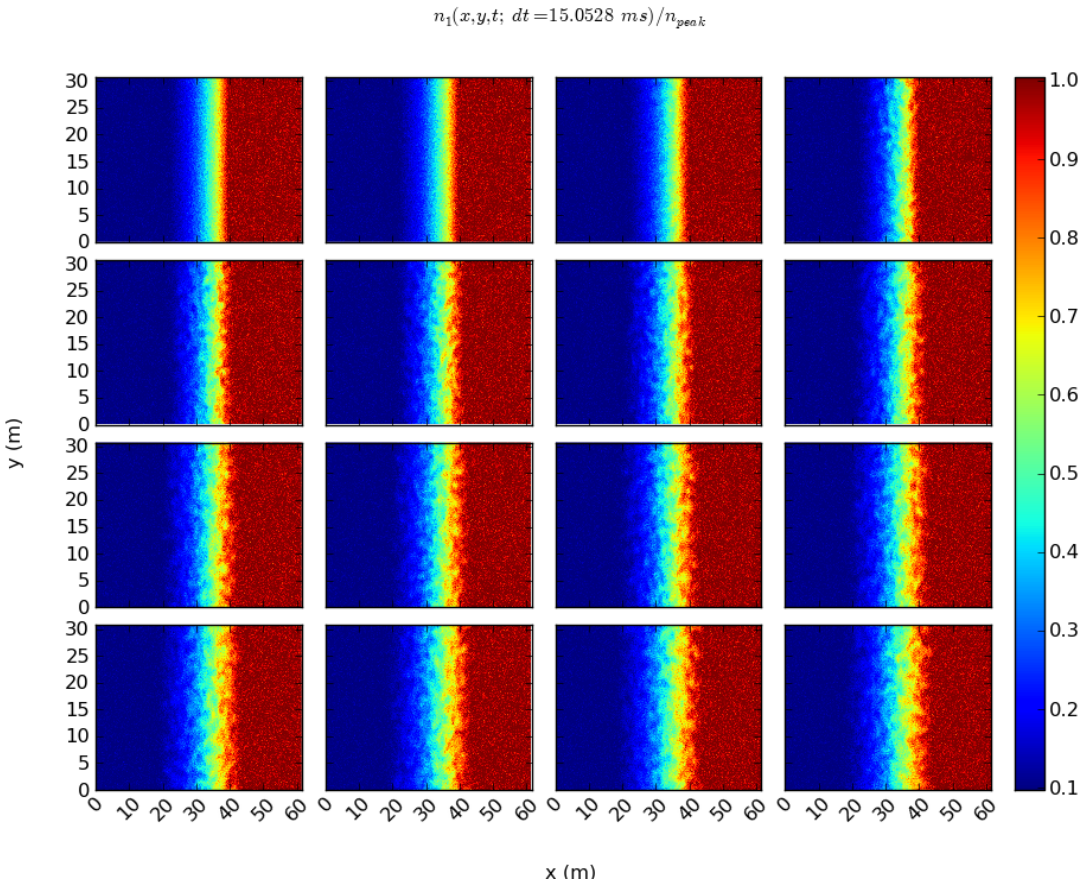

Figure 1: The ion density as a function of time, for a simulation with the parameters listed in Table 1. Time progress from left to right and top to bottom, and each frame shows high density (red) on the right and low density on the left, with a transition in the middle.

Early on in the simulation, regular, sinusoidal drift waves form as seen in the third pane in Figure 1). As time progresses, the linear process gives way to a non-linear turbulent dynamics, still localized to the region with the highest gradient. Surprisingly, the turbulence takes the form of eddies. A visual inspection of density perturbations suggests that the longest wave lengths have the largest growth rates, and a spectral analysis confirms that the instability consists of modes whose wave lengths are larger than 1 m.

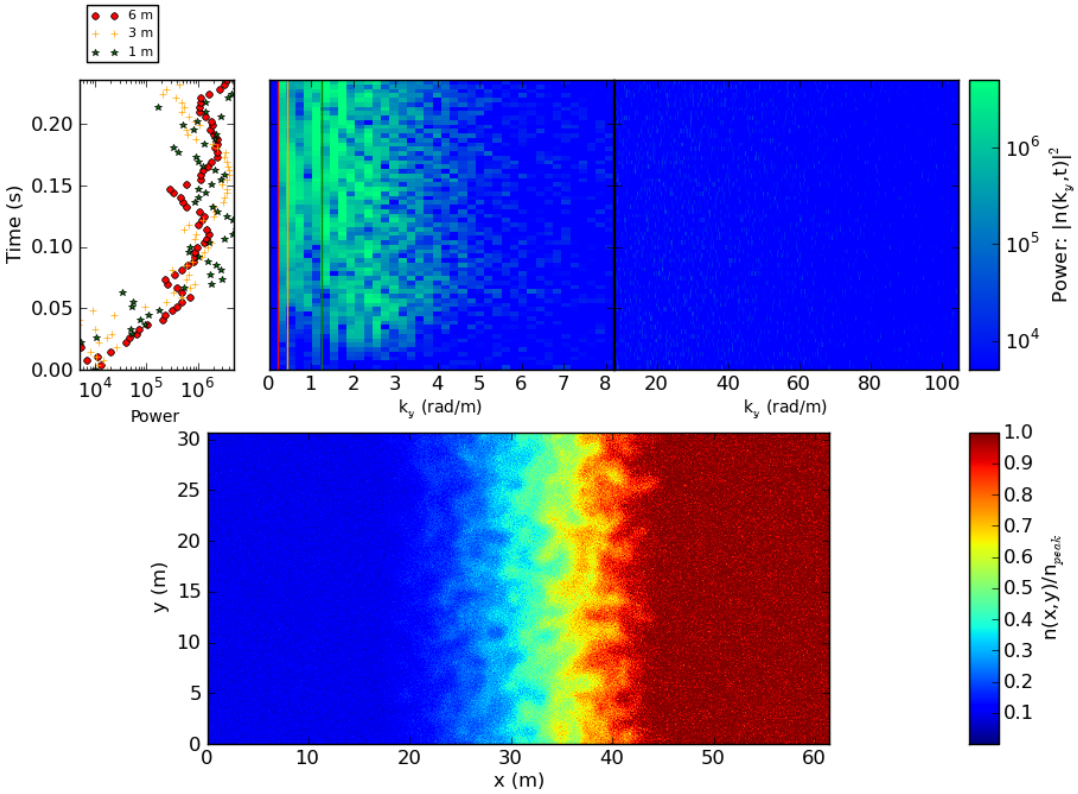

Figure 2: A spectral decomposition of the ion density shown as k_y vs time for $k_x = 0$.

Instability Growth and Saturation Figure 2 presents the amplitude of each k_y ($k_x = 0$) mode as a function of time, confirming that waves smaller than 1 m (a numerical limitation???) are effectively stable. It also shows in the left most plot that 1, 3 and 6 m waves grow simultaneously, with a similar growth rate.

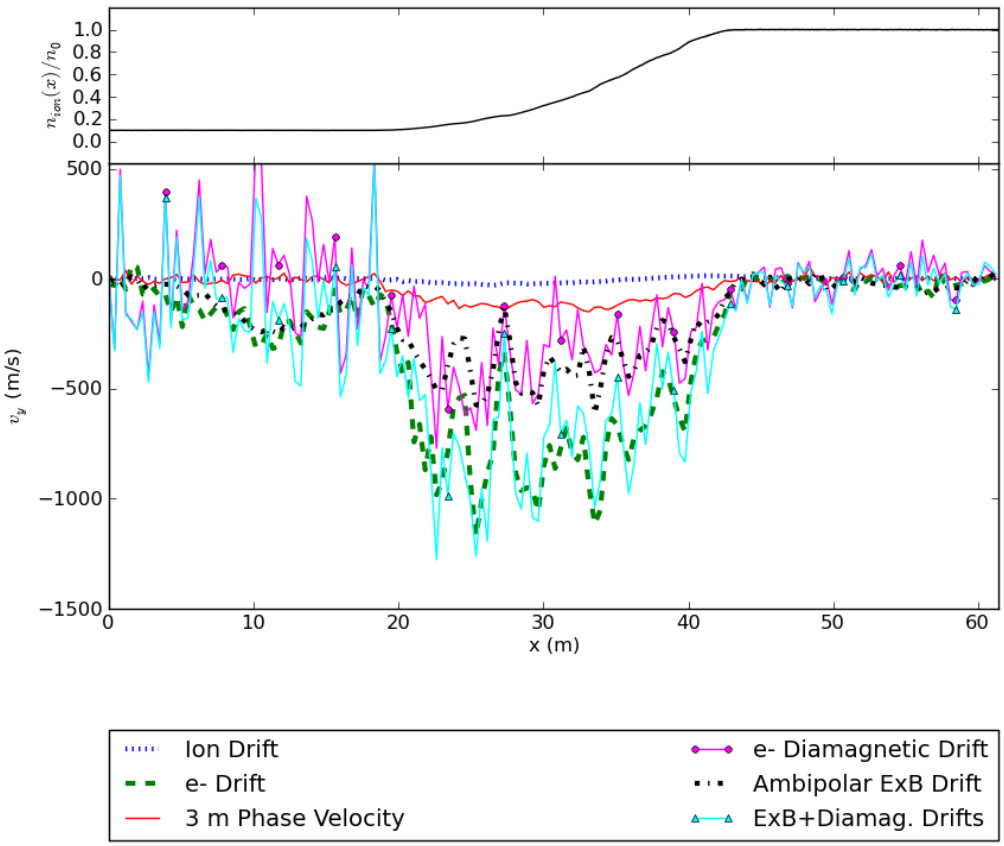

Figure 3: Physical and theoretical drifts as a function of the gradient direction (x) and averaged in the perpendicular direction (y).

The diamagnetic "drift" results from more particles gyrating in the higher density region, so that on average more ions move vertically while on average more electrons descend. We start our particles, however, with zero drift, and through the conservation of momentum in a collisionless plasma, the ions do not drift significantly in the actual simulations. On the other hand, the electrons drift with twice their expected velocity. The extra driver takes the form of an anomalous ambipolar field that develops to counter the ions response to a pressure driven Lorentz force, and thus the field helps effectively conserve momentum. On the other hand, the *ambipolar*-E×**B** drift is coincident with the electrons diamagnetic drift, and the electrons combined drift is twice as fast. If we initialize the particles with their corresponding drifts at t=0, then the ambipolar field

does not develop, but the particles still have a relative drift equal to the difference between their diamagnetic drift velocities. The instability progresses with the ions and at velocities smaller than the ion acoustic speed.

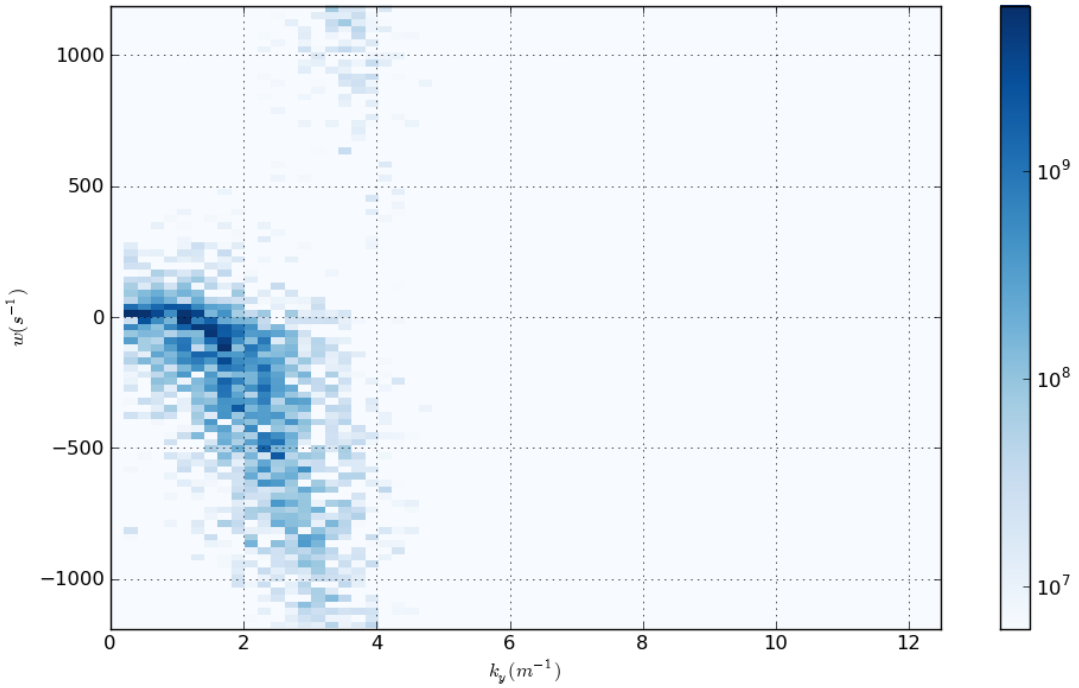

Figure 4: $n(k_y, \omega)$, the spectra for the ion distribution.

By investigating the density irregularities in Fourier space, we can identify trends that may suggest a named instability and the results at fixed wave length are comparable to the coherent echoes measured by ionospheric radars. Figure 4 presents such an analysis, showing the ion density as a function of k_y and ω. Its interesting to see that for small k_y, these small wave length modes have insignificant amplitudes, which is equivalent to that which is plotted in Figure 2. Also of interest is the dispersion curve for the modes with wave lengths larger than 1 m ($k_y \approx 6.3$; the frequency (ω) has a k_y^2 dependence, similar in nature to diffusion ($\nabla^2 n \rightarrow k^2 n$). Hysell and Kelley

[1997] suggested that the small scale waves are likely damped by diffusion, and such a process would have a power spectrum comparable to those measured by rockets and satellites. Since there are no collisions in these simulations, classical diffusion is not possible, but the resulting dynamics has a diffusion-like behavior that is consistent with the analysis of Hysell and Kelley [1997].

We investigated a range of gradients that produced these instabilities, and we found that for gradient length scales larger than 22 m, the instability did not form. This is at least half as long (50 m) as the steepest gradients measured in situ. This may suggest that these steep gradients are transient in CEIS, and this instability provides the mechanism for rapidly dissipating such steep gradients. The simulated instability quickly grows and saturates (see Figure 2) within a fraction of a second (.1 to .5 seconds, depending on the gradient strength). The turbulent dynamics facilitates the dissipation of such density gradients. In CEIS, the large scale background gradient (along with other forces) drives the growth of large scale ($>$ 1 km) structures that develop progressively steeper gradients until this small scale drift wave instability can rapidly grow and dissipate the medium-scale (100-1000 m) waves.

Boundary conditions, simulation size and electron mass This grant supported several key improvements to our simulation code that enabled us to study much larger, non-periodic simulations. We implemented a Message Passing Interface (MPI) parallel field solver, extending an existing serial version of the code [Birdsall and Langdon, 1991, Austin et al., 2004]. This allowed us to efficiently deploy our simulator with as many as 16384 processors. This parallelization is essential to try to simulate as broad a range of length scales as possible, and since the lower end of the range (approximately 1 cm) is fixed by numerical requirements, the added parallelization is the only way to reach the scales relevant for this study. The non-periodic conditions allow for several possible field and particle-injection boundary conditions.

For the field, Dirichlet ($\phi = 0$), Neumann ($\mathbf{E} = 0$), or Open ($\phi(\infty) = 0$) boundary conditions are available, and the particles are injected from a fixed flux or reflected at the boundary to maintain a fixed density and temperature. The system responds to excess change, so it is essential to use the correct boundary conditions, otherwise instabilities tend to develop on the boundary. Our experimentation with various combinations concluded that either Dirichlet or Neumann boundary

conditions provided the most stable representation of the electric potential, and while both injection and reflection particle boundary conditions provide similar results, reflection boundary conditions are less likely to result in charge build up on the boundaries.

For our studies, we investigated a range of gradients, and in comparison studies, we maintained all parameters except for the initial density profile. The distance over which the density changed remained fixed as did the peak density, so the lowest density changed with the gradient strength. Could it be that by having a gradient length scale longer than the distance over which the density changed affect the nature of the instability? For example, our densities changed over 15.5 m in most simulations, but we studied gradient length scales as much as 30 m. For these conditions, no waves developed, so is this due to the limited range? When we extended the range to 60 m, we still found that the waves were stable, from which we are able to confidently conclude that the cutoff for instability growth is approximately 22 m. While we would ideally wish to study much larger systems, we found our limited size did not prevent us from performing informative simulations.

Another parameter that could influence our simulations is the electron mass, which is artificially increased in the simulations to decrease the severity of certain numerical requirements. Upon lowering the mass to value approaching the true electron mass, the simulation results remained qualitatively the same. One key difference is a subtle increase in the growth of very short wavelength (< 0.5 m) modes, but the longest wavelength (1 to 6 m) modes grew at the same rate and saturated at the same amplitude. We conclude that kinetic effects dissipate the smallest wavelength modes in the larger-mass simulations, and these effects are dependent on the electron mass. The qualitative finding that the largest waves grow due to the gradient does not change. We are still exploring which kinetic process specifically contributes to the decay of the smallest modes in these simulations.

Finally, we considered the implications of using a regular grid, in space and time, and we were conscious that frequently these numerical approximations lead to numerical instabilities that are challenging to distinguish from physical processes. Not only do all essential physical time (plasma oscillation period, electron gyro period, etc) and length (e.g. Debye length) scales need to be resolved, they must be resolved several times over. Specifically, the simulation parameters resulted in a relative large electron cyclotron frequency (all though smaller than the physical frequency),

and the simulations that did not sufficiently resolve the entire gyration ultimately lead to heating. Just resolving this cyclotron frequency leads to a 1000 K rise in the temperature, but this heating was eliminated if the time step became 1 percent of the gyration period. This of course made each calculation 100 fold more expensive than originally perceived, but that is the cost of such reliable results.

We also explored developing a parallel quasi-neutral hybrid solver. Using the assumptions $n_i \equiv n_e$, $\nabla \cdot J = 0$, and inertialless electrons, the electron momentum equation is solved for the electric potential. Making numerical approximations leads to a non-normal matrix form that is slow to solve, but more importantly, the problem scales poorly. In spite of employing parallel matrix solvers, the code only scaled to 10's of processors, much less than the pure-PIC implementation.

3 dimensional simulations For our 3D simulations, we studied a system with simulation box dimensions 120 m by 60 m by 30 m for the magnetic field ($\mathbf{B}$), density gradient, and perpendicular directions respectively. Perpendicular to $\mathbf{B}$ these conditions are identical to those chosen for the 2D simulations, and all but the gradient direction are treated with periodic boundary conditions. We found very little density perturbations with wave vector components parallel to $\mathbf{B}$, but this may have been limited by two factors. First it is expected that the instability along $\mathbf{B}$ should develop much longer wavelength modes, and the simulation box dimensions along $\mathbf{B}$ may be too small to resolve the fastest growing parallel modes. Secondly, the development for all modes parallel to $\mathbf{B}$ is likely slower than the perpendicular direction. With this in mind, we feel confident that the 2D simulations, which produce nearly identical results, provide a good representation of, at least, the instabilities development-time dynamics.

2D bubble We also explored the development of drift waves for a circular density depletion, that is a miniature spread-F bubble. We employed periodic boundary conditions for both directions, but otherwise the plasma parameters are the same as used above. In the intermediate region, the gradient is constant, as opposed to the exponential transition (to impose a constant gradient length scale) used in the non-periodic simulations presented above. This results in a pressure that decreases away from the depletions center, and therefore the instability grows predominantly in the

lower density end of the gradient. Otherwise the dynamics is similar, shown in a different format in Figure 5. Since the pressure is stronger near the center, the electrons drift faster around the bubble, and ultimately this faster drift induces the slowly propagating waves to travel slightly more quickly in the center as well. The difference produces a spiral pattern, but it also leads to turbulence sooner in the center. The challenge with periodic simulations is that the driving density gradient dissipates before the instability can completely saturate. This problem, however, reinforces the conclusion that the steep gradients used in these simulations are not observed because they are transient in the F-region.

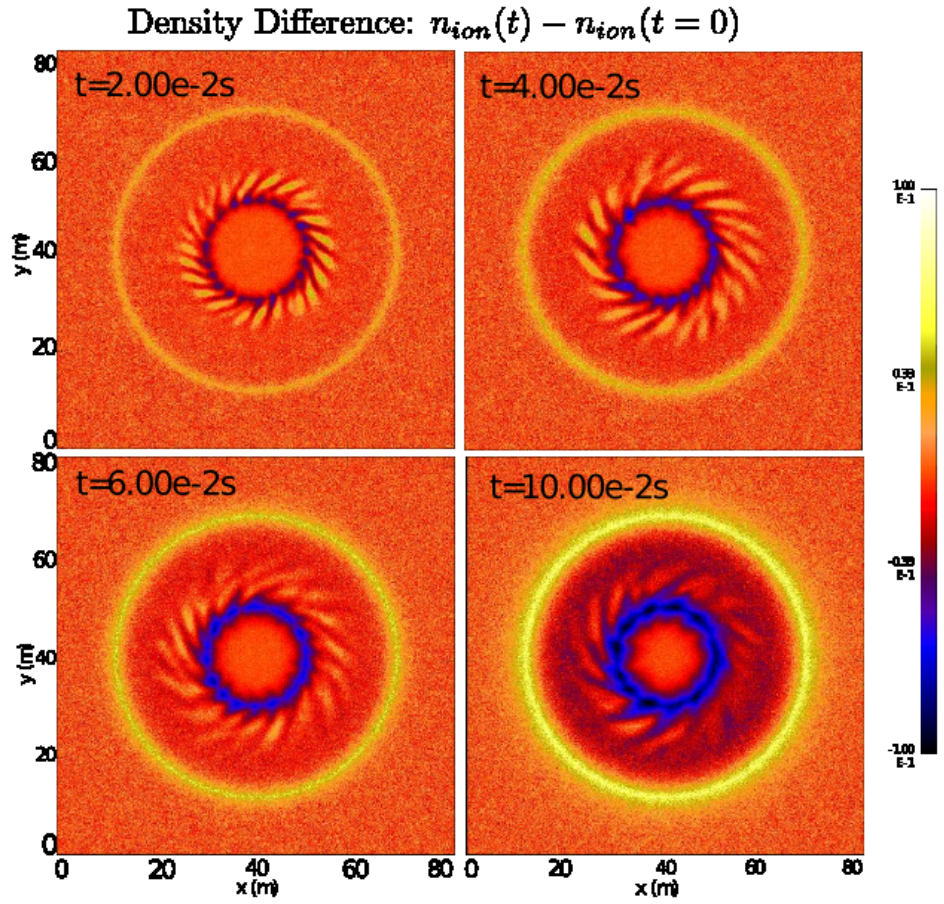

Figure 5: The density difference $(n(t) - n(t = 0)$ for a periodic, circular density depletion.

We also briefly investigated the effect of an ambient electric field on the instability's development, because satellites, such as C/NOFs, have measured electric fields associated with the walls

of the bubbles. Figure 6 shows a simulation with a 10 mV electric field pointing downward (-y direction), and this results, as may be expected, in an asymmetric development of the instability. On the right edge of the bubble, the background electric field adds constructively with the ambipolar field which develops to counter and ion diamagnetic drift. This leads to a larger clockwise electron drift, at least on the right hand wall. On the opposite edge, the fields add destructively, and the electrons experience the drift of an effectively much weaker density gradient. Therefore the instability is nearly stabilized on the left wall, and any growth occurring on the right edge is undone on the left edge as the waves propagate around the bubble. Unfortunately this configuration is transient as the periodic boundary conditions cannot maintain the intermediate scale gradient and the stronger instability facilitates faster dissipation of the initial structure.

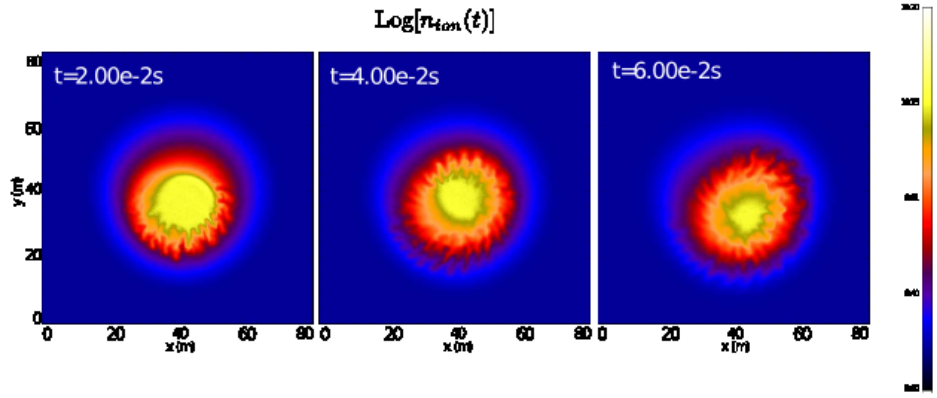

Figure 6: Bubble with Efield

3 Summary

The goal for this project was to investigate the small scale dynamics of CEIS. We performed a series of 2 and 3 dimensional PIC simulations investigating the effect of strong density gradients on a collisionless plasma. The resulting drift wave instabilities produced irregularities of similar length scale as those observed with coherent echo radars. At a maximum, a gradient length scale of 22 m was required to produce the small scale irregularities, and all larger values resulted in stable dynamics. This gradient length scale represents a steeper gradient than the steepest value

(approximately 50 m) typically observed with in situ measurements. We conclude that a simple drift wave instability is sufficient to explain the development of small scale irregularities as they quickly dissipate the steepened structures that drive their growth. Our investigations using 3D simulations produced dynamics similar to the 2D simulations in the plane perpendicular to the magnetic field. This validates the results of 2D simulations, at least for the early development of the instability. This work supports the theory that large scale CEIS dynamics progressively produces steeper and steeper structures on the intermediate scales, which ultimately are dissipated through a drift wave instability.

References

T. M. Austin, M. Berndt, and J. D. Moulton. A memory efficient parallel tridiagonal solver. Technical Report LA-UR 03-4149, Mathematical Modeling and Analysis Group, Los Alamos National Laboratory, Los Alamos, NM, 2004.

C. K. Birdsall and A. B. Langdon. *Plasma Physics Via Computer Simulation*. Adam Hilger, 1991.

Y. S. Dimant and M. M. Oppenheim. Ion thermal effects on E-region instabilities: linear theory. *Journal of Atmospheric and Solar-Terrestrial Physics*, 66:1639–1654, November 2004. doi: 10.1016/j.jastp.2004.07.006.

S. Peter Gary. *Theory of Space Plasma Microinstabilities*. Cambridge University Press, 1993.

J. D. Huba and S. L. Ossakow. On the Generation of 3-m Irregularities During Equatorial Spread F by Low-Frequency Drift Waves. *J. Geophys. Res.*, 84(A11):6697–6700, 1979. ISSN 0148-0227. URL `http://dx.doi.org/10.1029/JA084iA11p06697`.

J. D. Huba and S. L. Ossakow. On 11-cm irregularities during equatorial spread F. *J. of Geophys. Res.*, 86:829–832, February 1981a. doi: 10.1029/JA086iA02p00829.

J. D. Huba and S. L. Ossakow. Diffusion of small-scale density irregularities during equatorial spread F. *J. Geophys. Res.*, 86:9107–9114, October 1981b. doi: 10.1029/JA086iA11p09107.

D. L. Hysell and M. C. Kelley. Decaying equatorial ¡formula¿F region plasma depletions. *J. Geophys. Res.*, 1022:20007–20018, September 1997. doi: 10.1029/97JA01725.

D. L. Hysell, C. E. Seyler, and M. C. Kelley. Steepened structures in equatorial spread F. 2: Theory. *J. Geophys. Res.*, 99:8841–8850, May 1994. doi: 10.1029/93JA02960.

M. C. Kelley, C. E. Seyler, and S. Zargham. Collisional interchange instability. II - A comparison of the numerical simulations with the in situ experimental data. *J. Geophys. Res.*, 92:10089, September 1987. doi: 10.1029/JA092iA09p10089.

M. Singh and E. P. Szuszczewicz. Composite equatorial spread F wave number spectra from medium to short wavelengths. *J. Geophys. Res.*, 89:2313–2323, April 1984. doi: 10.1029/JA089iA04p02313.